Inspiration on Graphs

Baylor Fox-Kemper
GEOL2300

- A Favorite

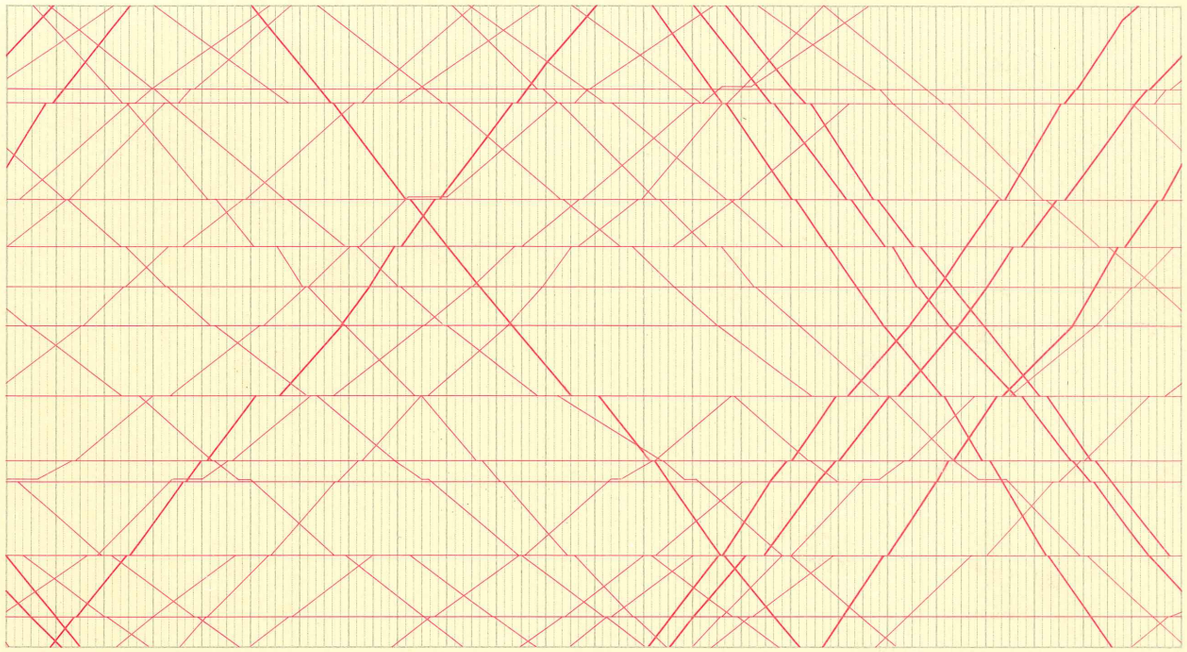

SECOND EDITION

The Visual Display of Quantitative Information

EDWARD R. TUFTE

A great example:
C.J. Minard as reproduced in
E.J. Marey, La Méthode Graphique (1885)

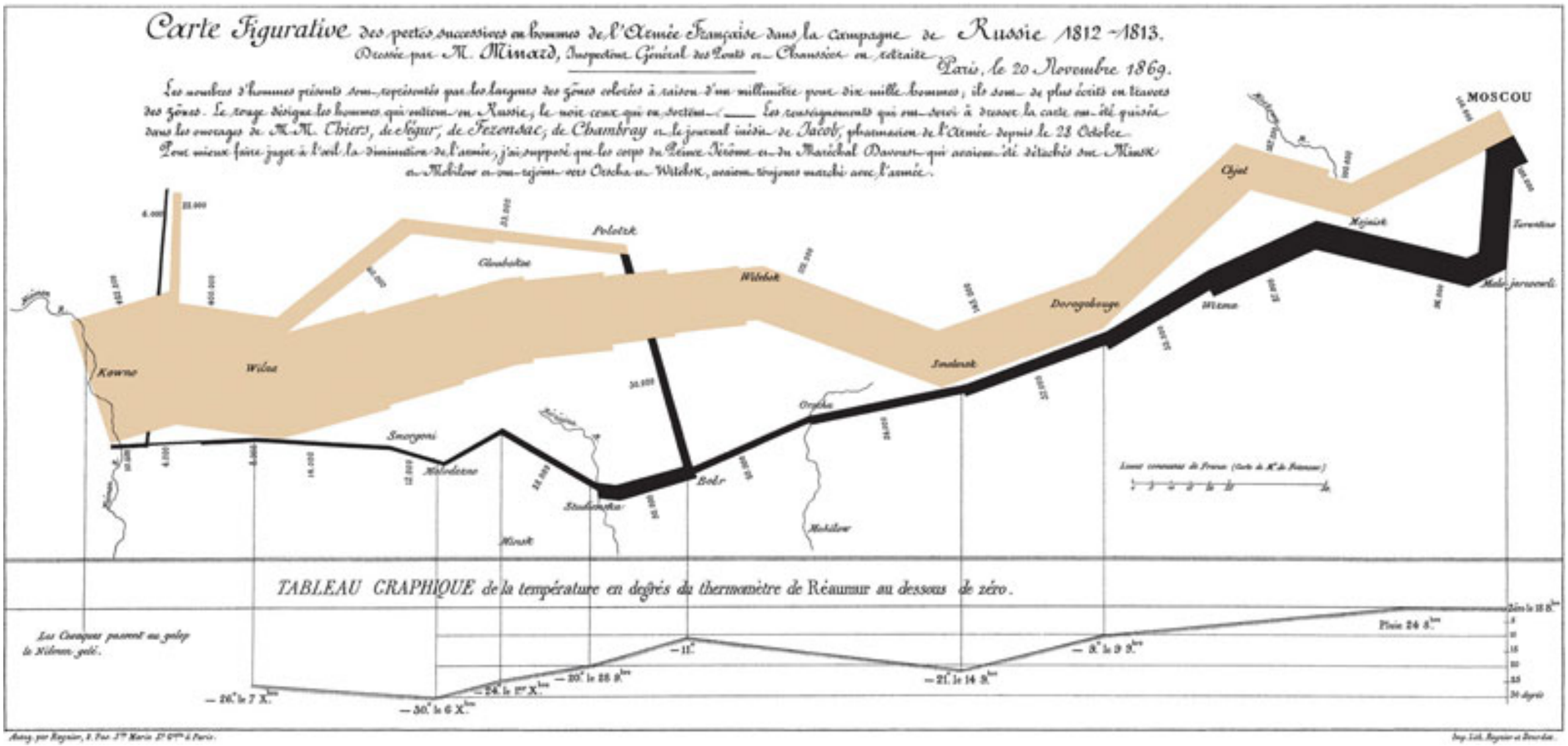

Avoiding Dimensional Constraints

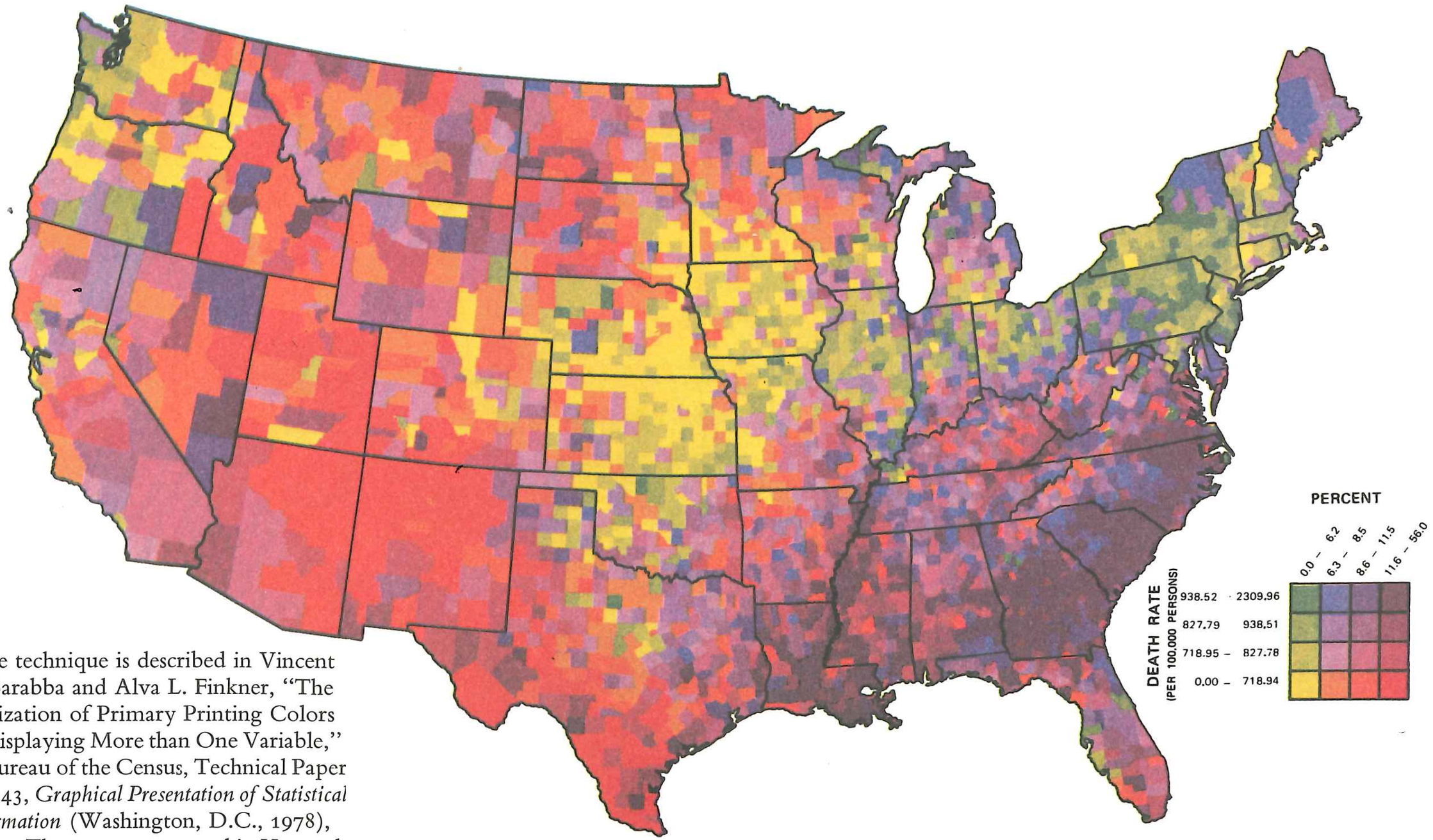

[4]The technique is described in Vincent P. Barabba and Alva L. Finkner, "The Utilization of Primary Printing Colors in Displaying More than One Variable," in Bureau of the Census, Technical Paper No. 43, *Graphical Presentation of Statistical Information* (Washington, D.C., 1978), 14–21. The maps are assessed in Howard Wainer and C. M. Francolini, "An Empirical Inquiry Concerning Human Understanding of Two-Variable Color Maps," *American Statistician*, 34 (1980), 81–93.

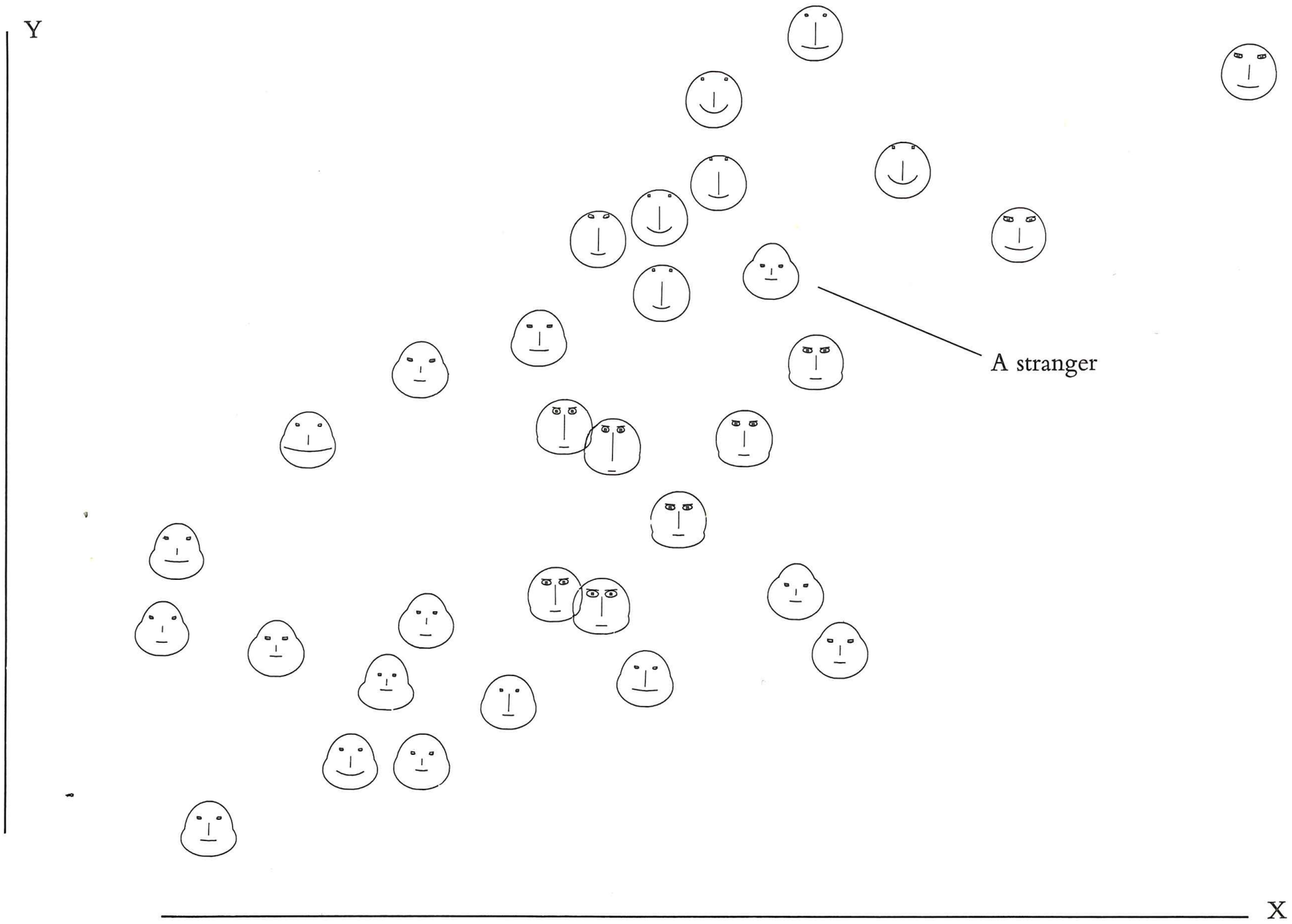

[3] Herman Chernoff, "The Use of Faces to Represent Points in k-Dimensional Space Graphically," *Journal of the American Statistical Association* 68 (June 1973), 361–368. For an application of faces located over two dimensions, see Howard Wainer and David Thissen, "Graphical Data Analysis," *Annual Review of Psychology*, 32 (1981), 191–241.

With cartoon faces and even numbers becoming data measures, we would appear to have reached the limit of graphical economy of presentation, imagination, and, let it be admitted, eccentricity.

Another Inspiration:
Jon Corum, 13pt.com, nytimes.com

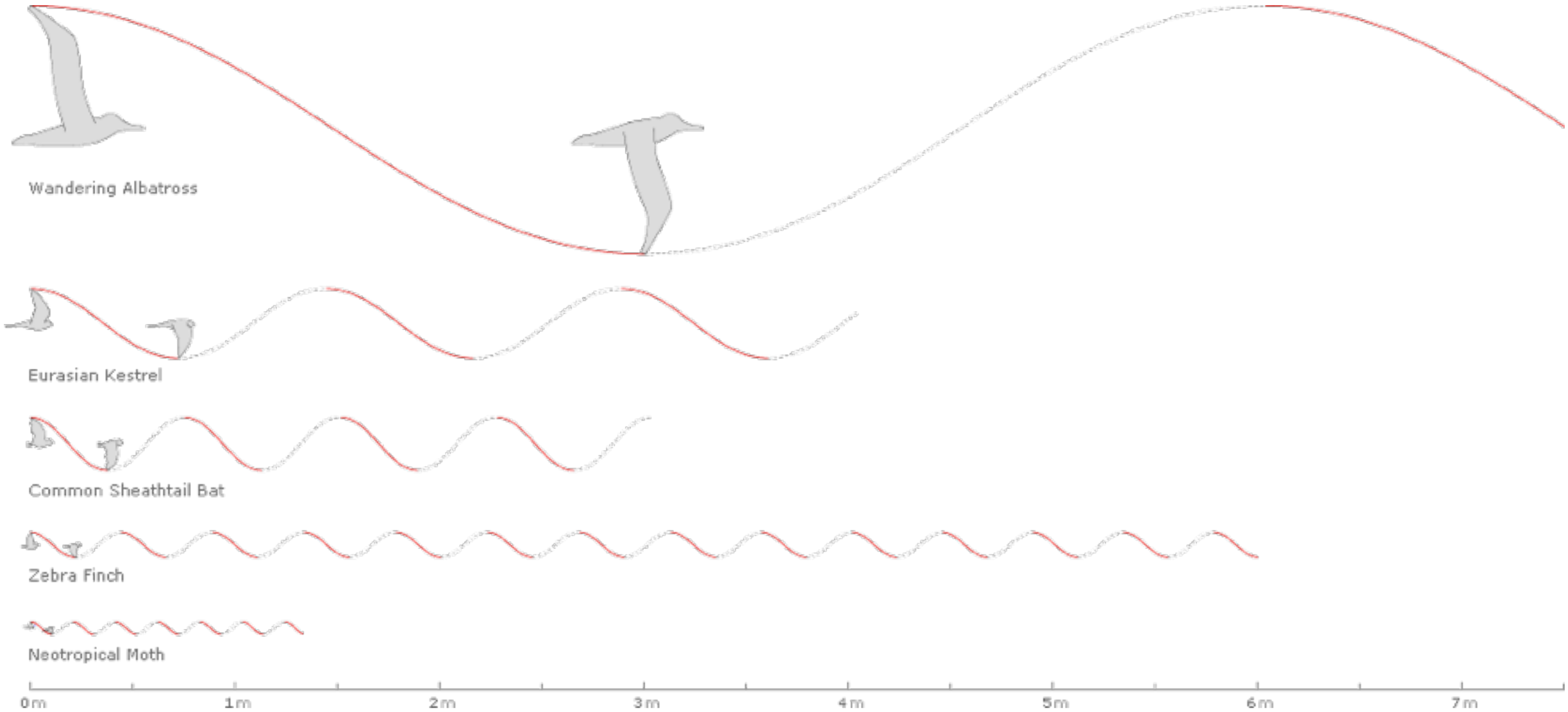

Still, this tells us nothing about Strouhal numbers.

Inverting and superimposing all 42 wavelengths on a common origin gives some sense of the range of the data sample:

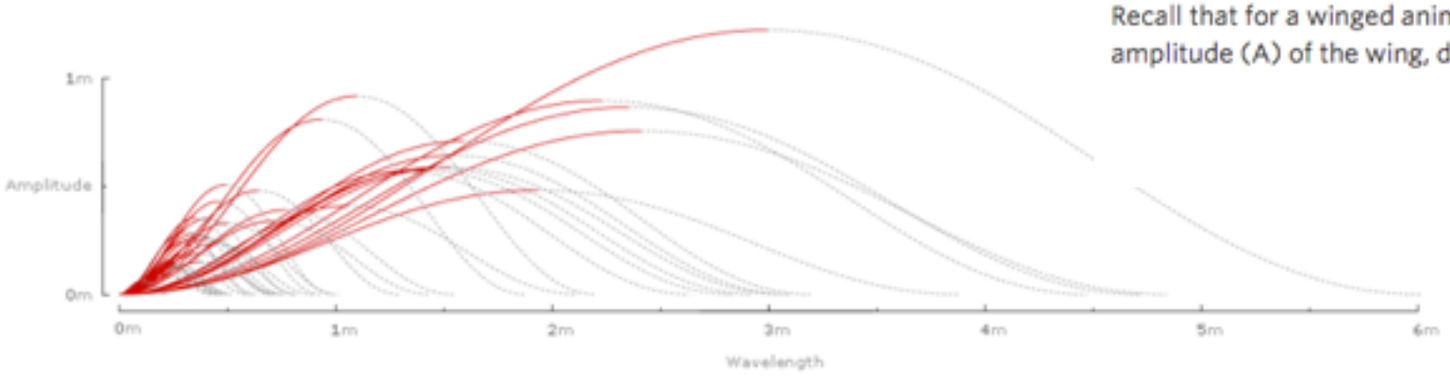

Recall that for a winged animal, the Strouhal number is the ratio of the frequency (f) of wing strokes, times the amplitude (A) of the wing, divided by the animal's forward speed (U):

$$\frac{f\,A}{U}$$

Plotting the rise and run of each wave gives a chart of Strouhal numbers for all 42 species:

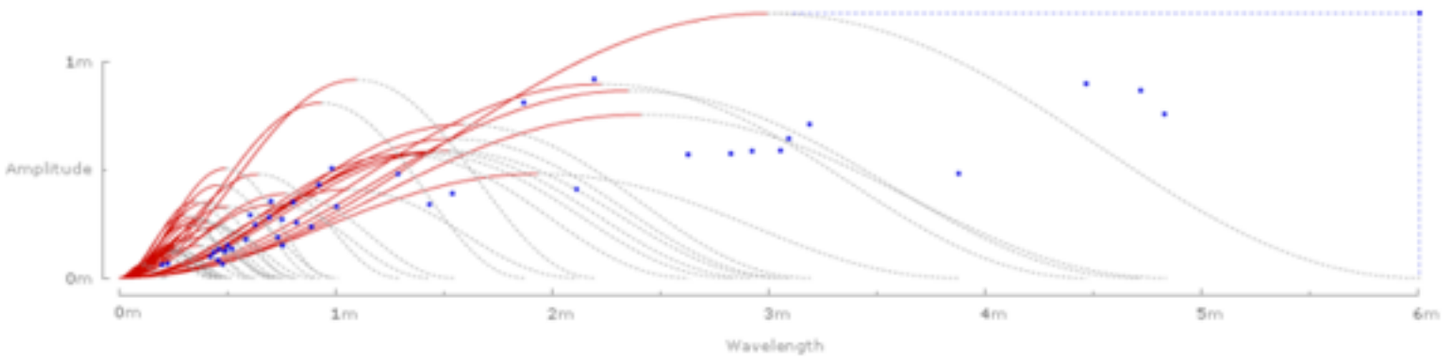

For the 22 species of birds:

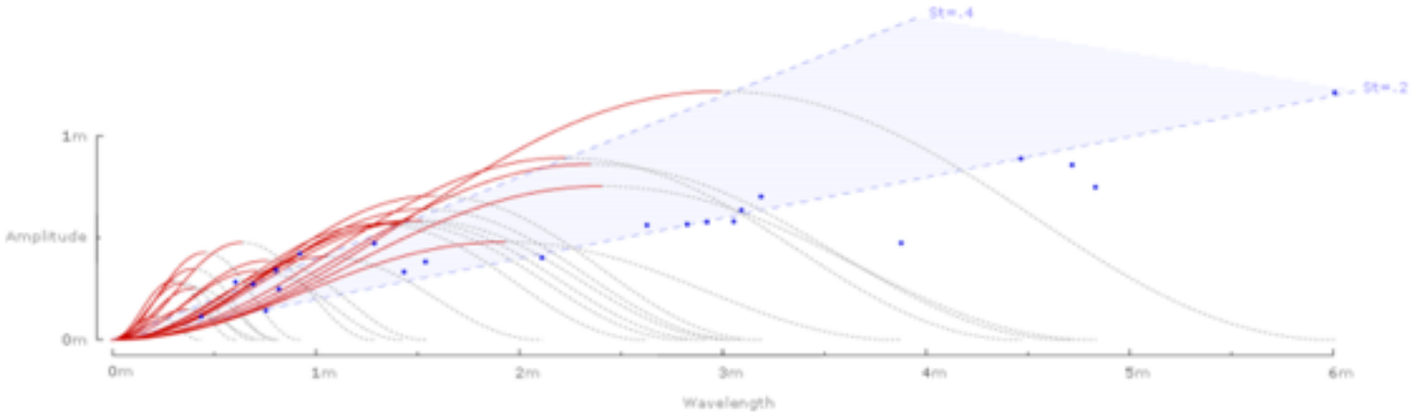

For the 20 species of bats:

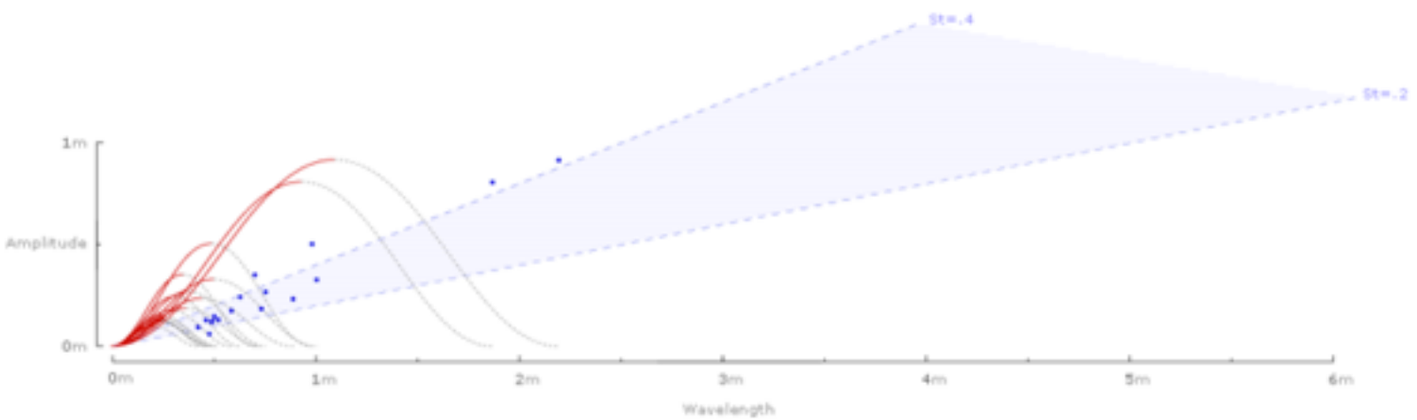

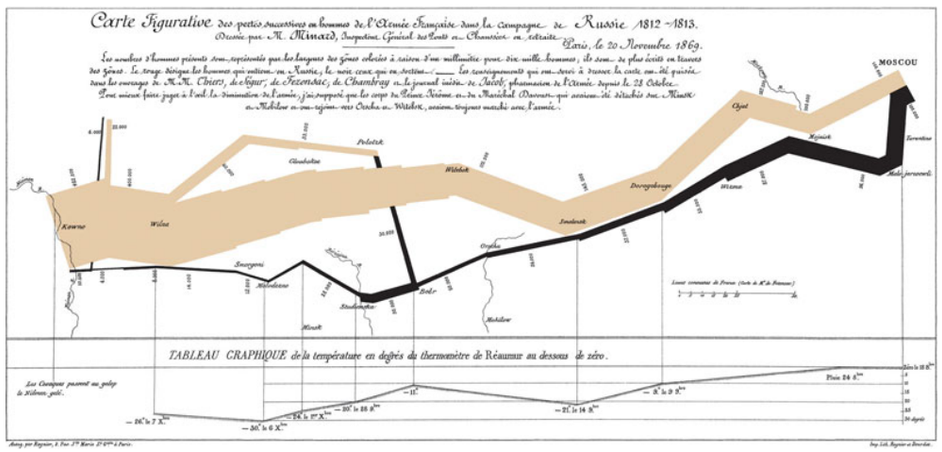

A condensed Lecture by Jon: http://style.org/tapestry/

Reconstructing a Bike Crash

A reporter crashed his bicycle near the end of a long ride, but was unable to recall any details of the crash. Below, a figurative map shows the start of his ride and the 20 minutes before the crash, using data retrieved from the bike's GPS device.

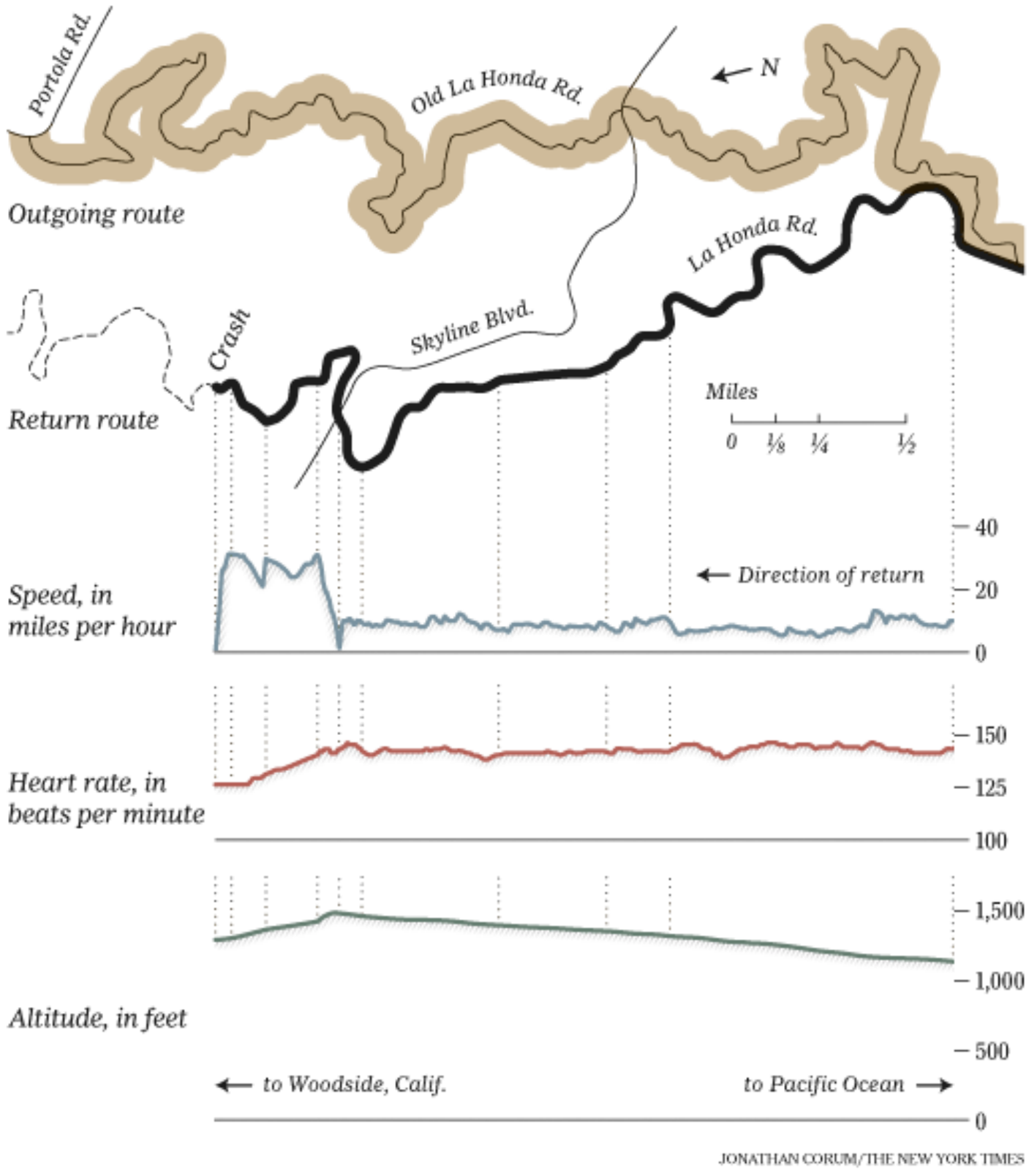

Some of my own favorites:

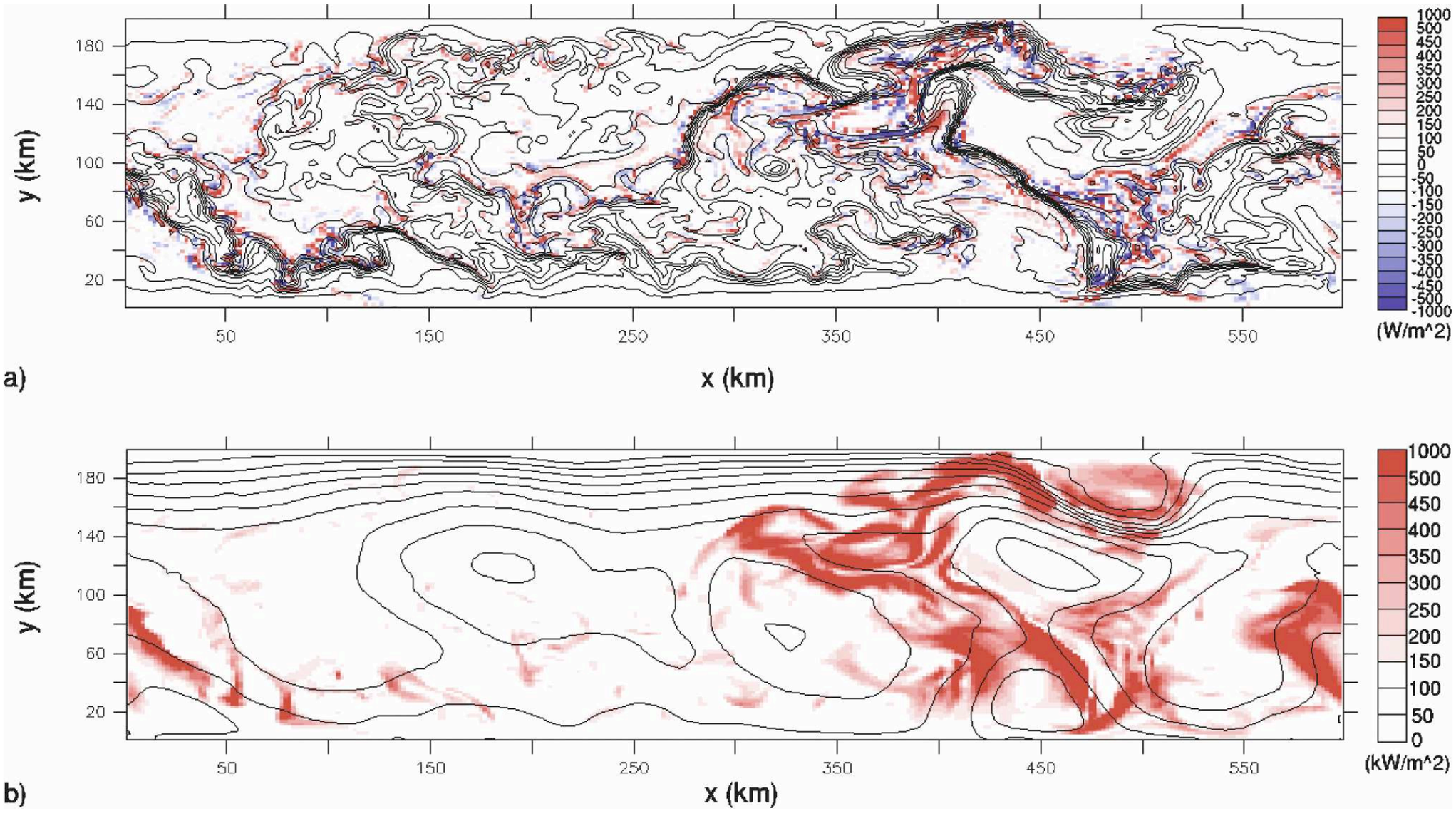

FIG. 1. Contours of temperature at (a) the surface and (b) below the ML base in a simulation with both mesoscale eddies and MLEs (0.2°C contour intervals). Shading indicates $w'b'$ in (a) and $|\mathbf{u}'_H b'|$ in (b) at 20-m depth, the depth at which eddy fluxes are largest.

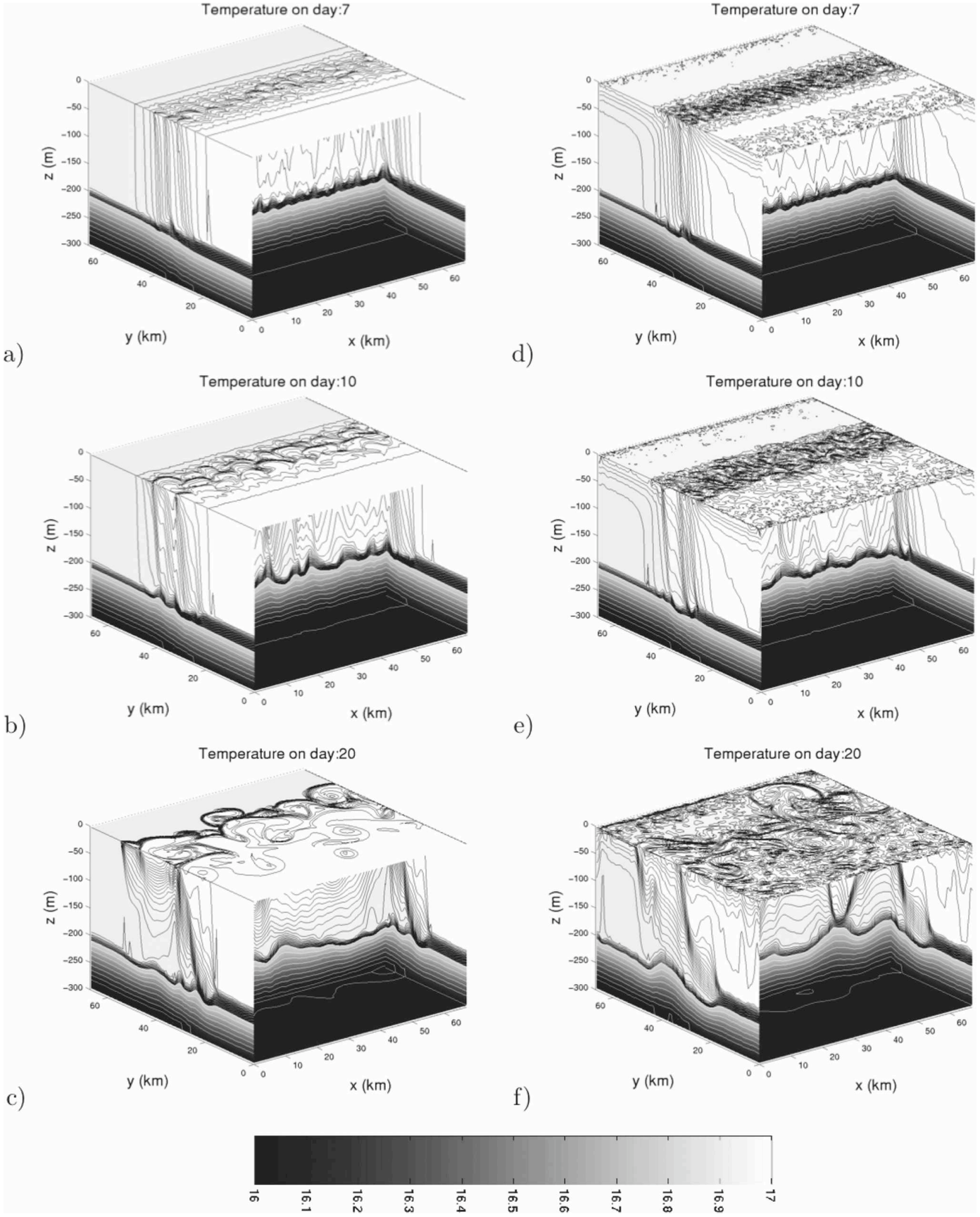

FIG. 2. Temperature (°C) during two typical simulations of a ML front spinning down: (a)–(c) no diurnal cycle and (d)–(f) with diurnal cycle and convective adjustment. (Black contour interval = 0.01°C; white contour interval = 0.1°C.)

(a)
x 10^-7
$\overline{v'b'}$
Snapshot
(b)
x 10^-9
$\overline{w'b'}$
Snapshot
(c)
R_{11}
Snapshot
(d)
R_{12}
Snapshot
(e)
R_{21}
Snapshot
(f)
R_{22}
Snapshot

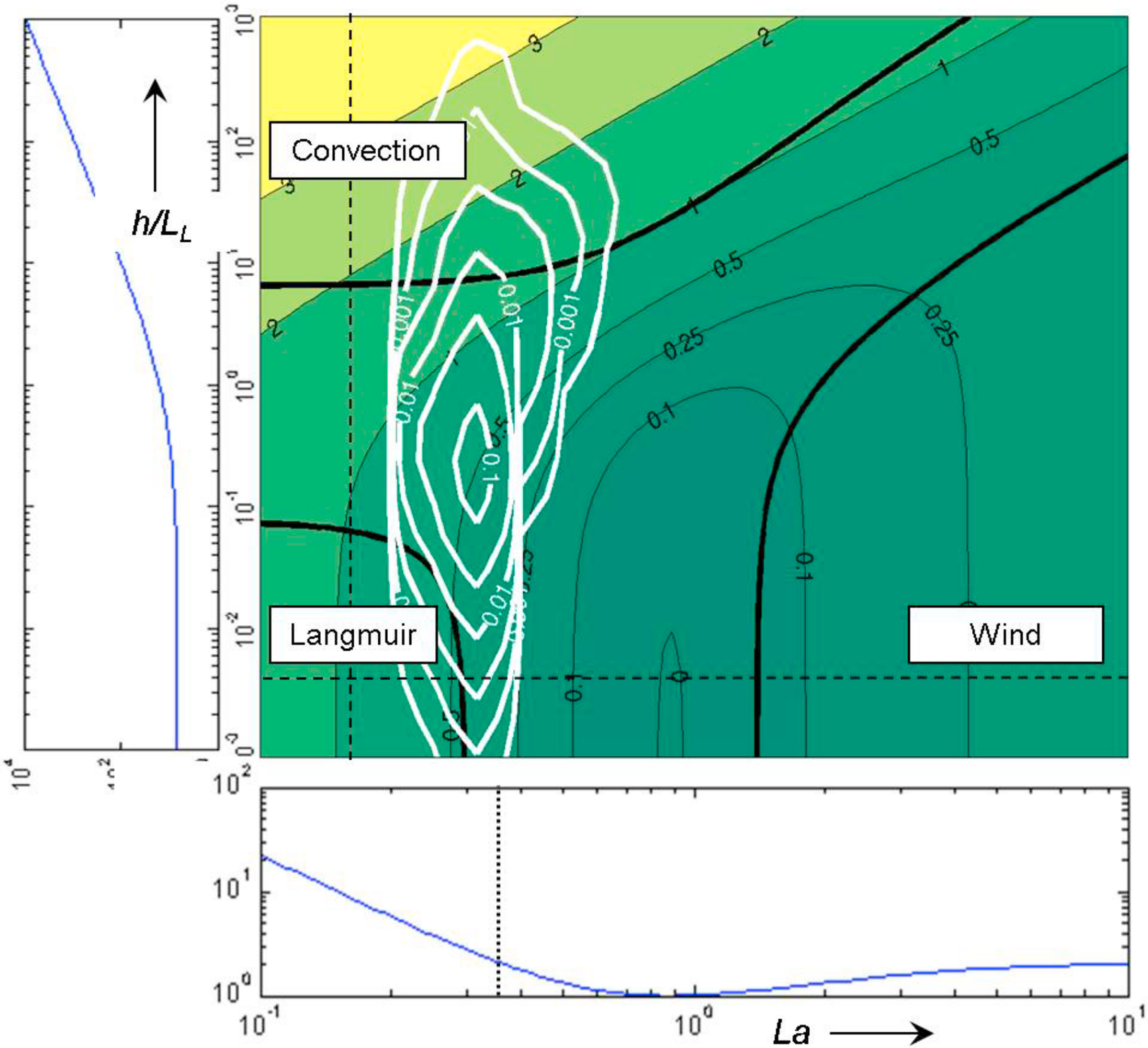

S. E. Belcher, A. A. L. M. Grant, K. E. Hanley, B. Fox-Kemper, L. Van Roekel, P. P. Sullivan, W. G. Large, A. Brown, A. Hines, D. Calvert, A. Rutgersson, H. Petterson, J. Bidlot, P. A. E. M. Janssen, and J. A. Polton. A global perspective on Langmuir turbulence in the ocean surface boundary layer. Geophysical Research Letters, 39(18):L18605, 9pp, September 2012.

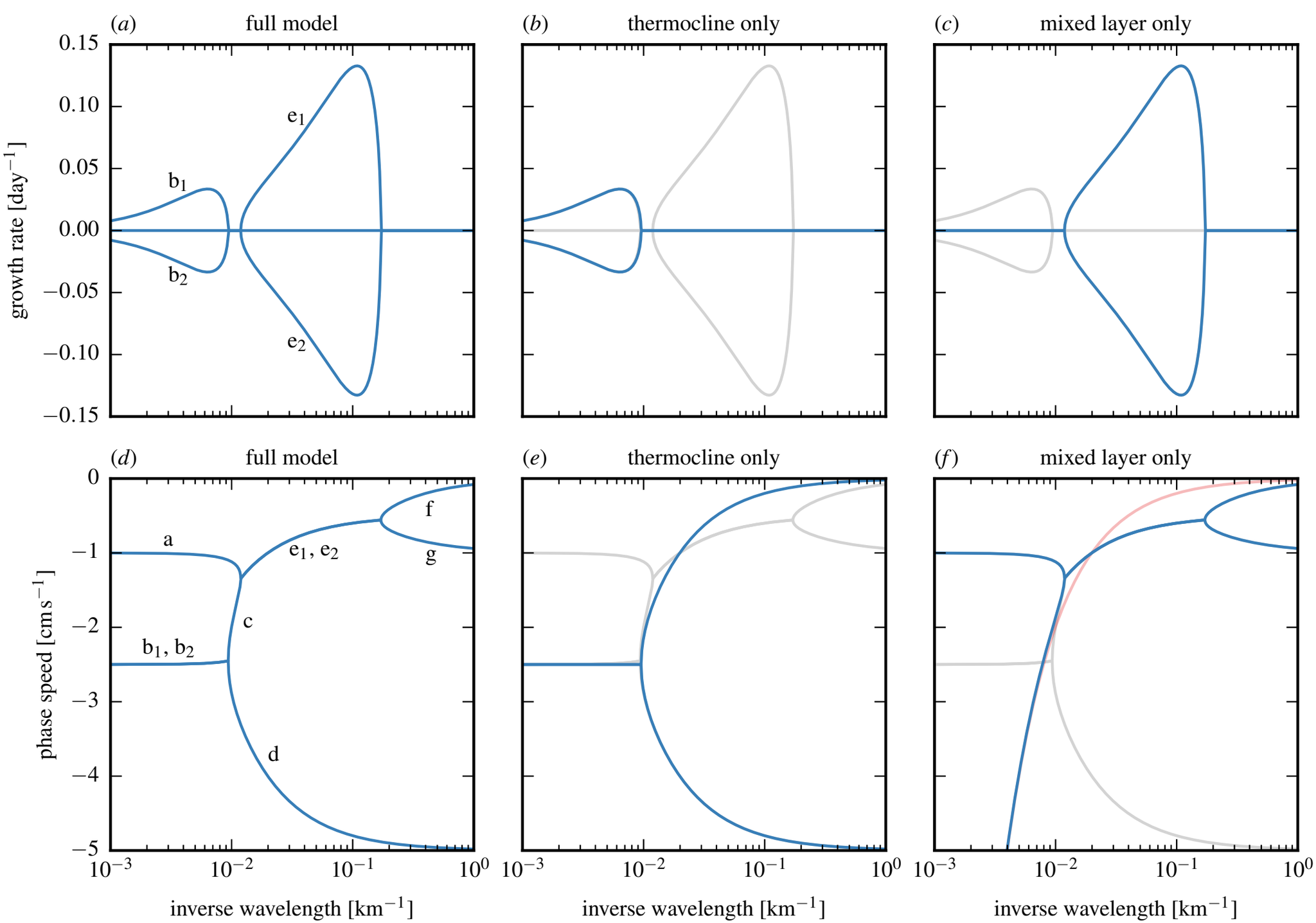

FIGURE 5. Linear stability analysis of the model equations. (*a*) growth rates and (*d*) phase speeds of the full model, (*b*) growth rates and (*e*) phase speeds of the thermocline-only model, (*c*) growth rates and (*f*) phase speeds of the mixed-layer-only model. Growth rates and phase speeds are shown in blue; the growth rates and phase speeds of the full model are overlaid for reference in gray. The phase speed of a surface edge wave is given in faint red in (*f*).

J. Callies, G. Flierl, R. Ferrari, and B. Fox-Kemper. The role of mixed layer instabilities in submesoscale turbulence. Journal of Fluid Mechanics, November 2015. In press.

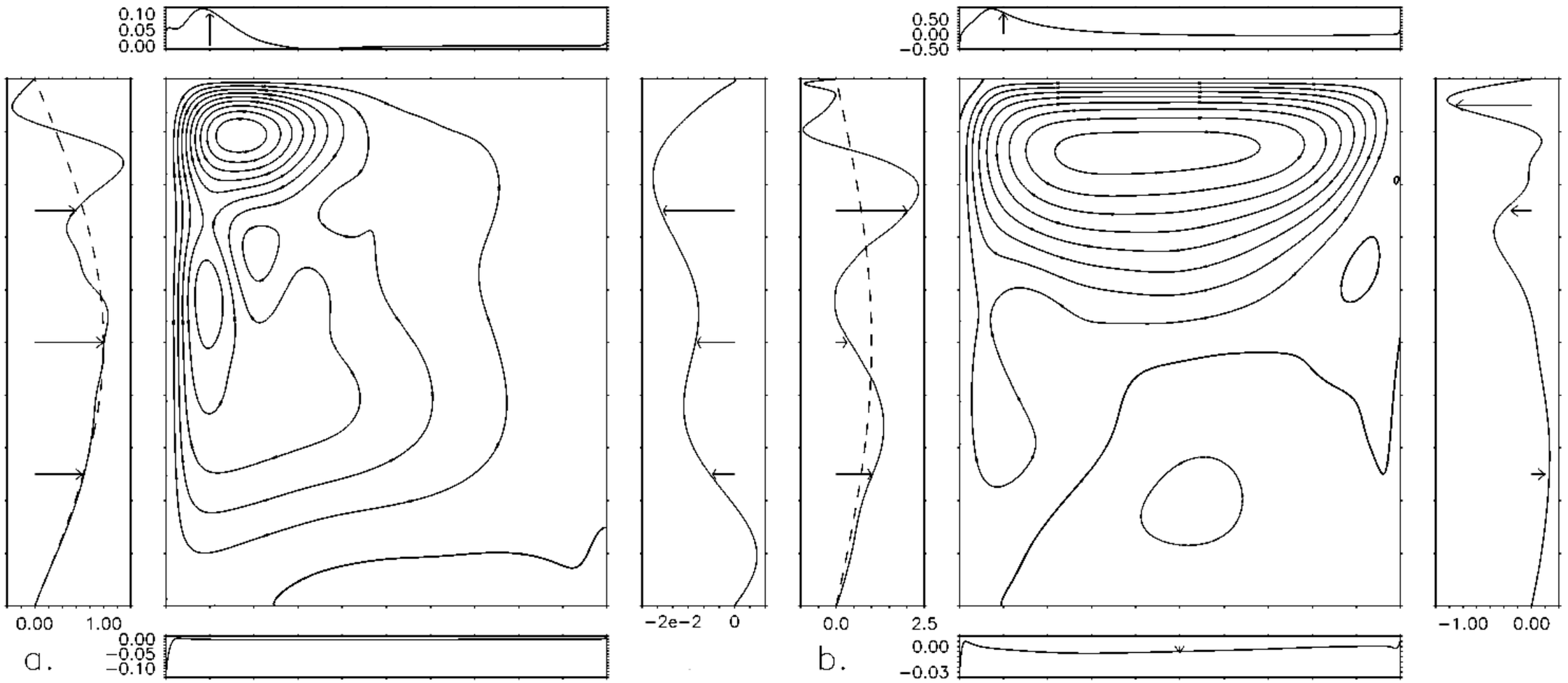

Figure 8. Maps of the normal frictional flux through each of the boundaries for (a) the western-intensified $Re_b = 0.25$, $Re_i = 5$ calculation and (b) the inertially-dominated $Re_b = 5$, $Re_i = 5$ calculation (on right). The four plots surrounding each contour plot indicate the frictional flux through the nearest boundary to each box ($-\delta_M^3 \nabla\zeta$) as a function of distance along the boundary. The flux through the western boundary needed to remove the wind vorticity input at the same latitude is overlaid with dashed lines. Arrows denote the direction of the frictional flux of positive vorticity. Note that the scales of the flux plots are different.

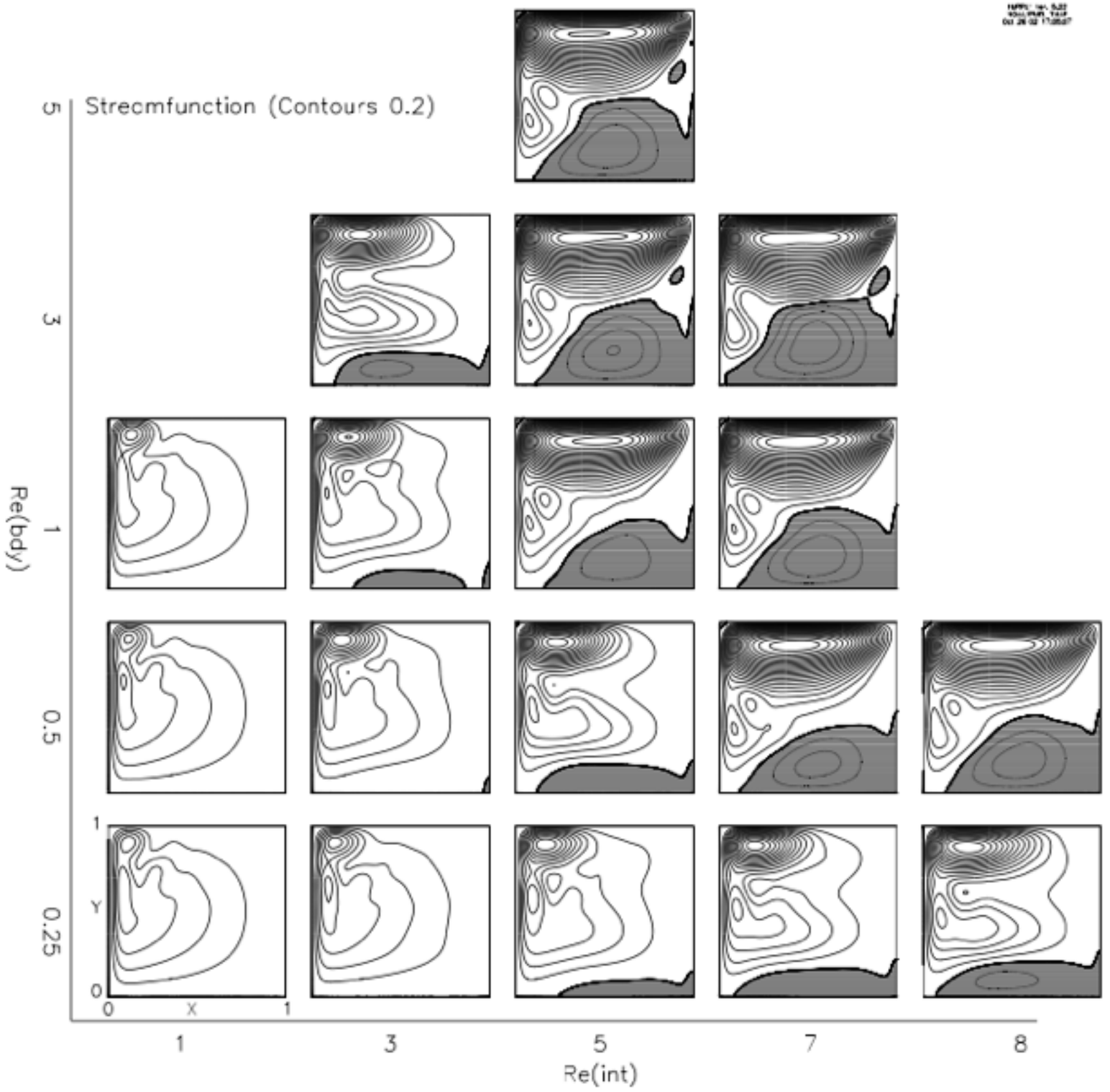

Figure 2-2: Collage of contours of the time-mean streamfunction for different values of Re(int) and Re(bdy). The contour interval is 0.2 in units where 1 is the maximum of the Sverdrup solution. Regions of negative streamfunction are shaded.

B. Fox. Eddies and Friction: Removal of Vorticity from the Wind-Driven Gyre. Ph.D. Thesis. MIT/WHOI, 2003-06, 2003.